Distribution Agreement

In presenting this thesis as a partial fulfillment of the requirements for a degree from Emory University, I hereby grant to Emory University and its agents the non-exclusive license to archive, make accessible, and display my thesis in whole or in part in all forms of media, now or hereafter now, including display on the World Wide Web. I understand that I may select some access restrictions as part of the online submission of this thesis. I retain all ownership rights to the copyright of the thesis. I also retain the right to use in future works (such as articles or books) all or part of this thesis.

Jennifer A. McGuire   April 10, 2018

Role of Glassy-Rubbery Interfaces on the Physical Aging of Glassy Polymer Thin Films

by

Jennifer A. McGuire

Connie B. Roth
Adviser

Department of Physics

Connie B. Roth

Adviser

Eric R. Weeks

Committee Member

Joyce Ho

Committee Member

2018

Role of Glassy-Rubbery Interfaces on the Physical Aging of Glassy Polymer Thin Films

By

Jennifer A. McGuire

Connie B. Roth

Adviser

An abstract of
a thesis submitted to the Faculty of Emory College of Arts and Sciences
of Emory University in partial fulfillment
of the requirements of the degree of
Bachelor of Sciences with Honors

Department of Physics

2018

Abstract

Role of Glassy-Rubbery Interfaces on the Physical Aging of Glassy Polymer Thin Films
By Jennifer A. McGuire

Polymers in a glassy state undergo physical aging. During this process they get denser and their volume decreases. We can measure this change in volume by measuring a change in film thickness. It is known that the glass transition temperature, T_g, the temperature at which a polymer transitions from a rubbery to a glassy state, is decreased at a glassy-rubbery interface. We also know there is a link between reduction in T_g and reduction in physical aging rate in single layer films. Previous work studied the physical aging of a glassy layer atop a rubbery layer and found no change in physical aging rate despite a reduction in T_g. They believed a possible explanation for this finding was that the free surface next to the glassy layer was canceling out the effect of the glassy-rubbery interface. My goal was to eliminate this effect by studying the physical aging of a glassy layer beneath a rubbery layer. Since the silica substrate has no effect on the polymer, this reduces the system to one interface. I studied bilayer systems with rubbery poly(n-butyl methacrylate) (PnBMA) atop glassy polystyrene (PS)

I found the physical aging rate of the glassy layer is not changed from bulk down to 142 nm of PS. Difficulty with measuring PS layers smaller than 142 nm beneath 400 nm PnBMA layers led to my decreasing the thickness of the PnBMA layer down to 150 nm. Bilayers with 150 nm PnBMA atop 150 nm PS produced aging rates in agreement with bulk data, so I was able to study PS layers of smaller thicknesses. There was no observable change in physical aging down to 57 nm of PS, but the measurements on 57 nm PS bilayers demonstrated issues with the PnBMA layer's sensitivity to the environment. Future work will include addressing ways to increase the PnBMA layer's resistance to changes in the environment and decreasing the PS layer thickness. Should a change in physical aging rate be observed in bilayers with smaller PS layers, future work will also study the T_g profile of the sample geometry used in this work.

Role of Glassy-Rubbery Interfaces on the Physical Aging of Glassy Polymer Thin Films

By

Jennifer A. McGuire

Connie B. Roth

Adviser

A thesis submitted to the Faculty of Emory College of Arts and Sciences
of Emory University in partial fulfillment
of the requirements of the degree of
Bachelor of Sciences with Honors

Department of Physics

2018

Acknowledgements

I would like to thank Eric Weeks and Joyce Ho for taking time out of their schedules to serve on my committee. Furthermore, I gratefully acknowledge all members of the Roth laboratory, especially Michael Thees and Benjamin Kasavan. I also thankfully recognize my family and friends, especially my parents, for all of their love and support. Above all, I would like to thank my advisor Connie Roth for her phenomenal mentorship. Without her, this work would not exist.

Table of Contents

Table of Figures

Chapter 1: Introduction and Background

Polymers are large molecules present in everything from DNA to Styrofoam to Plexiglass. They have many industrial applications and are very common in the manufacturing of newer and lighter technologies. Many industrial applications consist of multiple polymers adjacent to each other. One such example is HIPS, high impact polystyrene, which consists of a mixture of glassy polystyrene and rubbery polybutadiene. The addition of polybutadiene modifies the polystyrene's response to deformation and impact. HIPS is commonly used for refrigerator doors, plastic cups and toys. While glassy-rubbery polymer-polymer interfaces are very frequent in applications, not much is known about the local property changes these polymer-polymer interfaces have on the material. This work will focus on the effect of a glassy-rubbery polymer-polymer interface on the physical aging of a glassy polymer thin film. Physical aging is associated with numerous property changes as a function of time, including the densification of a polymer, which causes the polymer to become more brittle.

1.1: Glass Transition and Physical Aging

Polymers are extremely long molecules that exist primarily in two states, a glassy state and a rubbery state. In a rubbery state not far above the glass transition temperature, T_g, the polymer segments are free to move through cooperative segmental motion and exist in equilibrium. The rubbery state is shown as the red equilibrium liquid line in Figure 1. As the temperature of the polymer is reduced, the polymer segments rearrange themselves to accommodate the change in temperature and remain at equilibrium. However, at some point, the rate of cooling will outpace the rate at which those segments can rearrange, and the segments become primarily "frozen" in place, entering a glassy state. These glassy states are shown as the green and blue lines in Figure 1. The temperature at which this change from a rubbery to a glassy

state occurs is called T_g. The cooling rate affects the exact temperature at which the transition from a rubbery to glassy state occurs, as can be seen in Figure 1. A faster cooling rate results in a higher T_g because the temperature reduction outpacing the timescale of the rearrangement of the polymer segments occurs sooner. Below T_g, in the glassy state, cooperative segmental motion becomes arrested, but there are still small amounts of local motion that occur to move the material towards an equilibrium state. This local motion gives rise to physical aging.
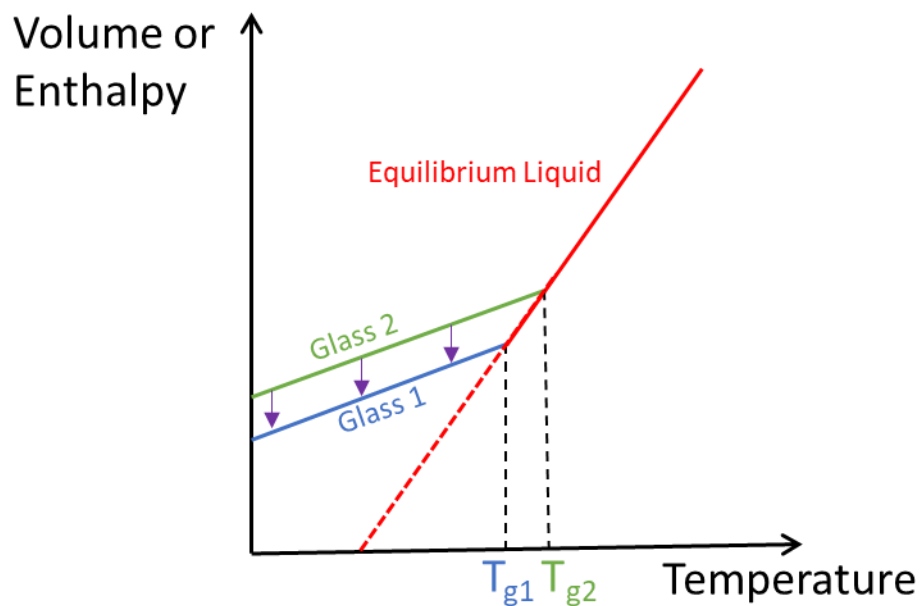
Figure 1. Illustration of the glass transition temperature, T_g, and the transition between the rubbery state and the glassy state.

Physical aging is the collection of behaviors in glassy polymers which change as a function of time at constant temperature and under no influence from other external conditions [1]. It encompasses a number of properties, including specific volume and enthalpy. The physical aging process is reversible if reheated above T_g, so it leaves no permanent chemical or physical changes in the material. One way to measure physical aging is to study the departure from

equilibrium δ, the excess specific volume normalized with respect to the equilibrium volume, where

$$\delta = \frac{v - v_\infty}{v_\infty} \qquad (1).$$

In Eq. (1) v is the volume of the film at a given time and v_∞ is the equilibrium volume. The volume relaxation rate, β, is defined to be [1]

$$\beta = -\frac{d\delta}{d\log(t - t_i)} = -\frac{1}{v_\infty}\frac{dv}{d\log(t - t_i)} \qquad (2).$$

β is also known as the physical aging rate and will be referred to as such throughout the rest of this work.

1.2 Ellipsometry

Ellipsometry can be used to measure the thickness of polymer films. Ellipsometry measures the change in polarization that occurs on reflecting visible light of wavelength $\lambda = 400 – 1000$ nm off a sample consisting of a polymer film atop a silicon substrate, as shown in Figure 2. The bulb emits visible light, which gets converted to linearly polarized light by the polarizer. The compensator is a quarter-wave plate which turns the linearly polarized light into elliptically polarized light. The elliptically polarized light is then reflected off the sample and passed through another polarizer (the analyzer). The light is dispersed onto a CCD detector array so that it can measure the range of wavelengths simultaneously. Those wavelengths are then interpreted according to a specified model of the sample.
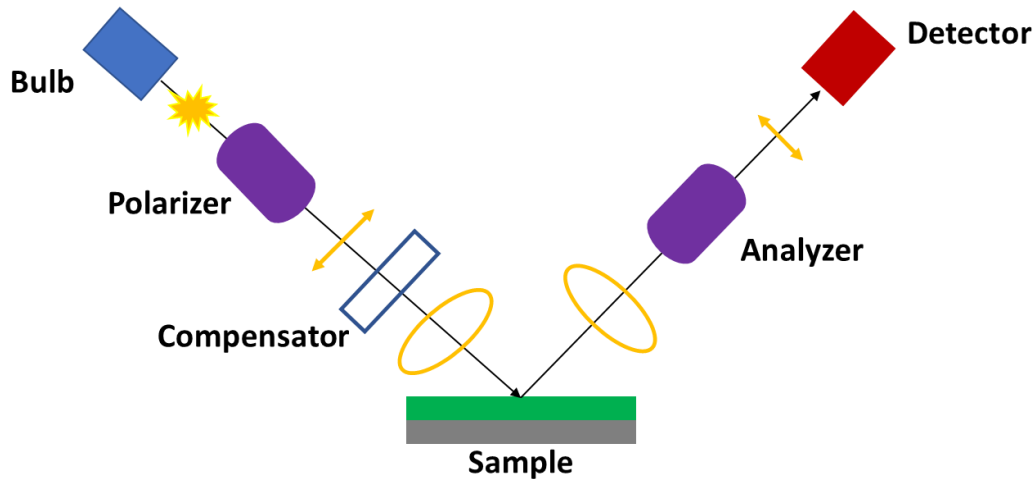
Figure 2. Diagram of ellipsometer.

Figure 3 shows the structure of a polymer film sample and the path of the beam from the ellipsometer traveling through the sample. The beam is both reflected back into the air and refracted into the polymer film as it crosses the air-polymer film interface. When that refracted beam comes into contact with the polymer film-SiOx interface, the beam is then both reflected and refracted. The refracted beam, again, is refracted and reflected at the SiOx-silicon interface. However, the refracted beam from the SiOx-silicon interface does not reach the other side of the silicon layer. The reflected beam leaving the sample is what gets received by the detector of the ellipsometer.
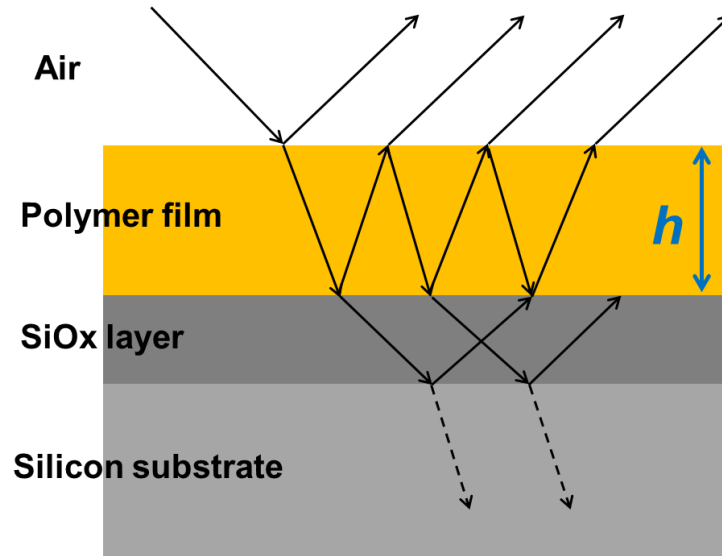
Figure 3. Structure of a polymer sample.

The signal recorded by the ellipsometer is the ratio of the reflected beam's polarization perpendicular (p) and parallel (s) to the plane of incidence and is given by [2]

$$\rho = \tan(\Psi)\, e^{i\Delta} = \frac{r_p}{r_s} \qquad (3)$$

where $\Psi(\lambda)$ and $\Delta(\lambda)$ are ellipsometry parameters. They are fit to a layer model of the film that uses Fresnel reflection coefficients to determine how the electric field changes upon reflection.

A Cauchy model is used to model the polymer index of refraction, n, [2]

$$n(\lambda) = A + \frac{B}{\lambda^2} + \frac{C}{\lambda^4} \qquad (4)$$

where A, B and C are fitting parameters. The Cauchy model is based upon the sample structure shown in Figure 3. Air is known to have an index of refraction of 1.00. The silicon substrate has a known $n(\lambda)$-$ik(\lambda)$ and absorbs ($k \neq 0$), so the light beam does not go all the way through the Si substrate. Silicon has a native silicon oxide (SiOx) layer atop it, and that layer is of known thickness with a known $n(\lambda)$. The $n(\lambda)$ of the polymer layer is measured, and the layer is fit to Eq. (4). From this fit model, the thickness of the polymer film, h, can be extracted.

Ellipsometry can measure changes in the thickness of films down to a hundredth of an

angstrom [3]. Therefore, ellipsometry has an extremely low relative error, meaning that once the

instrument is aligned, it can measure changes in thickness with a high degree of precision.

1.3 How Ellipsometry Measures Physical Aging

Because supported polymer films are confined to the substrate, the only direction of

contraction during physical aging is in the vertical direction. Therefore, the change in volume is

proportional to the change in film thickness, h, so v in Eq. (2) can be replaced with h to give

$$\beta = -\frac{1}{h_\infty}\frac{dh}{dlogt} \qquad (3),$$

where h_∞ is the equilibrium thickness of the film [3]. However, h_∞ must be extrapolated from the

equilibrium liquid state above T_g. This is typically done through a linear extrapolation of a $V(T)$

or $h(T)$ plot to the aging temperature, but it leads to large extrapolations and is not the only

method of estimating h_∞. In 2009 Baker et al. [3] developed a new streamlined procedure for

measuring physical aging using ellipsometry. They found they could accurately measure aging

rates by normalizing the thickness values to h_0, the initial thickness of the film,

$$\beta = -\frac{1}{h_0}\frac{dh}{dlogt} \qquad (4).$$

They compared Eq. (4) to Eq. (3) and other methods of calculating β from the literature for data

collected over 24 h using bulk polystyrene (PS) films for a variety of temperatures. Eq. (4) was

in good agreement with Eq. (3) and another literature method, indicating the validity of Eq. (4).

In an effort to maximize efficiency for measuring β, Baker et al. also compared various aging

times for measuring a bulk PS film using Eq. (4). Typically, 24 h has been regarded as sufficient

to measure physical aging, but a variety of aging times have been used in the literature. Upon

comparing aging times of 500 min, 360 min, 200 min and 120 min to 24 h, Baker et al. found

that for temperatures above 330 K (57 ºC) , all aging times produced similar aging rates, but for temperatures below 330 K, shorter aging times produced lower values of β. An aging time of 360 min was required to accurately measure β. Therefore, all physical aging measurements in this work were taken by measuring film thickness over a period of at least 360 min (most longer than 800 min) and using Eq. (4) to calculate β [3].

1.4 Local T_g in Thin Films

Polymer films begin to experience what is known as confinement when interfacial effects become important. One of the effects of confinement is the reduction in average T_g seen in thin films. There had been some debate about the connection between the length scale of the cooperatively rearranging region (CRR) and the length scale at which nanoconfinement effects are observed. In 2003, Ellison and Torkelson characterized the distribution of T_gs in PS films [4]. They measured the local T_g at the free surface of a PS film by creating a bilayer film of a pyrene-labelled PS layer and a bulk PS layer and measuring the T_g of the labelled layer using fluorescence. Fluorescence works because the excited state of pyrene is competing with the nonradiative decay that occurs by vibrational or other modes. As the temperature increases, the nonradiative decay increases, so the fluorescence decreases. This effect, combined with sensitivity of pyrene to local density provides the shift in temperature dependence of intensity at T_g used to measure local T_g. To measure the local T_g at the free surface, they varied the thickness of the pyrene-labelled surface layer in Figure 4(a) atop a 270-nm thick unlabeled PS film and measured the T_g of the surface layer.
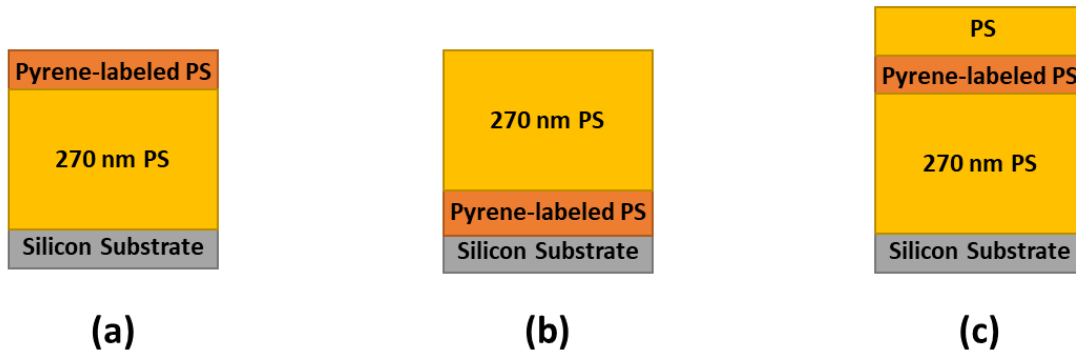
Figure 4. Sample structures used by Ellison and Torkelson.

They also studied a 3-layer model, shown in Figure 4(c), in which the pyrene-labelled layer was held at a constant thickness of 14 nm and embedded a variable distance from the top of the film, with a non-labeled PS layer above and below. They found the T_g of the free surface layers was reduced from bulk, not returning to bulk values until the 30-40 nm from the free surface. T_g varies smoothly with the thickness of the surface layer, indicating the segmental mobility near the surface is significantly faster than bulk. They also studied the local T_g near the substrate by using a bilayer film with a 12 nm thick pyrene-labelled PS layer below a 270-nm unlabeled PS layer, shown in Figure 4(b). They found the local T_g remained equal to that of bulk, indicating the substrate has little effect on the local T_g of the film. Their studies indicate a smooth gradient in cooperative dynamics and that the substrate and surface layer dynamics are important. They demonstrated that perturbed layers in a film affect other layers in the film to a lesser extent and the length scale of that effect is of primary concern.

For films of total thickness between 25 nm and 60 nm, the surface T_g is increased, measured using a surface layer of 14 nm. For films thinner than 25 nm, the T_g of the surface layer is comparable to that of the whole film. When films are less than 60 nm thick, the gradient is adjusted to accommodate the thinner film, but it always remains a smooth gradient. However,

when films are less than 25 nm thick, there is a single T_g, which is believed to be due to an insufficient length scale to create a smooth gradient in average cooperative dynamics. Overall, this shows that the distance over which an alteration in dynamics has an effect is on the order of several tens of nanometers and the effect of the enhanced surface-layer mobility is dependent on the level of nanoconfinement of the whole film. These findings provide an interesting basis for studying the dynamics related to T_g and physical aging.

1.5 Relationship Between T_g and Physical Aging

In 2010, Pye et al. found a reduction in physical aging rates in thin films (approximately 30 nm) at all temperatures [5]. For films of thickness greater than or equal to 100 nm, the physical aging rate was independent of film thickness, but there was a steady decrease in physical aging rate for films less than 100 nm corresponding to a decrease in film thickness. They thought this decrease might be explained by a shift in temperature dependence of the physical aging rate to lower temperatures corresponding to the shift in T_g seen in the work of Ellison and Torkelson [4]. However, the $\beta(T)$ curve was not simply shifted to lower temperatures; the physical aging rate of thinner films was reduced at all temperatures. Pye et al.[5] concluded this reduction in physical aging rates could be explained by a gradient in dynamics near the free surface, much like the gradient in dynamics responsible for reductions in T_g seen in thin films [4]. They fit the data with both a 2-layer model, comprising of a surface layer above a PS layer, and a gradient model. Both models produced equivalent depths to which the free surface affects the film.

1.6 Local T_g in PS/PnBMA Films

In addition to being reduced at the free surface of a film, the T_g of a polymer can be affected by the presence of another polymer. In 2015, Baglay and Roth studied the profile of the local T_g across a glassy-rubbery polymer interface [6]. They used PS and poly(n-butyl methacrylate) (PnBMA), which have a 80 ^{o}C difference in bulk T_g. PS has a T_g^{bulk} of 100 ^{o}C, and PnBMA has a T_g^{bulk} of 20 ^{o}C. The advantage of studying such a system is that the transition can be mapped from one well-defined T_g to another. For high molecular weight polymers, a stable well-defined polymer-polymer interface between PS and PnBMA has a width of 7 nm [7, 8], so it was initially thought that the transition from one T_g to the other would be on a similar length scale and symmetric. However, Baglay and Roth found that the local T_g takes approximately 350 – 400 nm to fully transition and that the profile is asymmetric towards the glassy PS side. The profile takes approximately 250 nm for local T_g to return to bulk on the PS side of the interface and approximately 150 nm for local T_g to return to bulk on the PnBMA side of the interface. This profile is clearly much larger than that anticipated by the width of the interface, indicating the polymer-polymer interface has a much longer ranged effect than previously believed.

1.7 Physical Aging Rate in PS/PnBMA Films

Previously Rauscher et al. studied the effect of an adjacent rubbery layer on the physical aging rate of a glassy polymer by measuring the physical aging rate of a bilayer film consisting of glassy PS atop rubbery PnBMA [8]. This work was done prior to that of Baglay and Roth [6]. Rauscher et al. [8] observed strong reductions in the average T_g of the PS layer consistent with both the free surface and PS/PnBMA interface speeding up the local dynamics. Based on the work of Pye et al. [5] linking a reduction in physical aging to a reduction in T_g, it was anticipated Rauscher et al. [8] would see a similar correlation in this system.

To study the ability to measure the physical aging rate of only the glassy PS layer when measuring the whole PS/PnBMA film by ellipsometry, they demonstrated that the thickness of the rubbery PnBMA layer remained constant throughout a physical aging run. Based on the stability of the thickness of the rubbery PnBMA layer, they concluded any change in film thickness must be due to the glassy PS layer, thereby allowing the measurement of β for the PS layer from the measurement of the whole film.

Multiple fitting models were used on the collected aging data for bilayer films [8]. The first involved fitting the thickness of the layer and A and B of the Cauchy model for both the PS layer and the PnBMA layer. In addition to having 6 fitting parameters, this method became problematic when the PS layer was significantly thinner than the PnBMA layer. The second method held the thickness and A and B parameters constant at bulk values for the PnBMA layer and fit the thickness and A and B parameters for the PS layer. This method gave less sample-to-sample variability and was most reliable for films with thin PS layers. Additionally, it was always consistent with the method based on total bilayer thickness. Due to its consistency and simplicity with fewer fitting parameters, this second fitting method was used for analyzing all data in their work.

Rauscher et al. found that varying the thickness of the PnBMA layer had no effect on the physical aging rate of the bilayer film [8]. They tested bilayers with PnBMA layers ranging in thickness from 45 nm to 1300 nm and found a consistent average aging rate of $\beta = (9.3 \pm 0.3) \times 10^{-4}$. In order to remain safely in the bulk region, the PnBMA layer was subsequently held constant at 500 nm. These results were as expected, since, due to being in the rubbery state at their aging temperature, the PnBMA layer should not have experienced physical aging. However, Rauscher et al. also saw no change in physical aging rate with varying thicknesses of

the PS layer. Bilayers with PS layers ranging in thickness from 86 nm to 580 nm were measured, and all had a consistent average aging rate of $\beta = (9.1 \pm 0.3) \times 10^{-4}$. These results were contrary to what would be expected based on the work of Pye et al. [5] because, despite a large reduction in average T_g of the PS layer, there was no reduction in physical aging rate. Rauscher et al. believed a possible explanation for these surprising results was that the effect of the free surface may have been canceling out the effect of the rubbery-glassy interface, thus showing no change in the physical aging rate.

1.8 Goal of Thesis

The goal of this thesis is to build upon the work of Rauscher et al. [8] to further examine the effect of an adjacent rubbery layer on the physical aging rate of a glassy polymer film. To address the concerns raised by the work of Rauscher et al.[8] and in light of later work done by Baglay et al. [6], I will be studying a system of a rubbery PnBMA layer atop a glassy PS layer. This system will eliminate the effect of the free surface on the physical aging rate of the glassy PS layer, ideally allowing me to study solely the effect of the rubbery PnBMA layer on the physical aging rate of the glassy PS layer.

Chapter 2: Experimental Methods

2.1: Sample Preparation

Four types of samples, all approximately 2 cm x 2 cm, were used in this work. The first sample was a piece of silicon with a 1000 nm thermal oxide layer (SiO_2/Si) used to measure instrument stability. This sample was purchased already prepared. The remaining three samples were polymer films spin-coated onto silicon wafers with 1.25 nm thick native oxide layers (SiOx/Si). The second sample type were polystyrene (PS) films. These were made with M_w = 2,000,000 g/mol (M_w/M_n = 1.30) PS from Pressure Chemical Co. via a 3% solution of PS in toluene spin-coated onto a silicon wafer which had previously been rinsed in toluene. These samples were annealed at 120 °C under vacuum for approximately 18 hours before use. The third sample type was poly(*n*-butyl methacrylate) (PnBMA) films. These were made with PnBMA with a M_w = 319,200 g/mol and M_n=123,900 g/mol from Scientific Polymer Products Inc. via a 4% solution of PnBMA in toluene and spin-coated onto a toluene-rinsed silicon wafer. These samples were annealed at 70 °C under vacuum for approximately 18 hours before use.

Bilayer samples were assembled as follows. The same PS used in single-layer PS samples was spin-coated onto silicon and annealed under vacuum at 120 °C for at least 18 hours. The same PnBMA used in single-layer PnBMA samples was spin-coated onto freshly-cleaved mica and annealed under vacuum at 70 °C for at least 18 hours. Following annealing the PnBMA film was floated onto the PS film by using the hydrophobic property of PnBMA and hydrophilic property of mica to separate the PnBMA film from the mica. The PnBMA film could then be placed onto the PS film, since the PS film would not separate from the silicon substrate in water. Each bilayer film was allowed to dry for at least 30 minutes prior to use. The final annealing of the sample was done during the first part of the ellipsometer aging protocol (to be discussed

below), where the sample was annealed at 120 ºC for 30 minutes. Some bilayer samples were

made by floating the PnBMA film onto PS without the separate annealing step on mica first.

These samples were annealed as a single bilayer at 80 ºC for at least 18 hours, and the final

annealing step was the same as for other bilayer samples. No differences were observed in the

measured aging rate.

2.2: Ellipsometer Aging Measurements

For all samples, a single temperature profile was used to measure physical aging.

Samples were heated to 120 ºC in 1 min, held at that temperature for 25 min then quenched

down past the desired aging temperature to 55 ºC in 30 s, resulting in a quench rate of 73 ºC/min.

Samples were held at 55 ºC for 0 min before being heated back to the desired aging temperature

of 65 ºC in 15 s and held at that temperature for an aging time. With the exception of the 1000

nm SiO_2/Si samples used to measure instrument stability and two PnBMA samples used to

measure PnBMA stability, thickness measurements were collected for 28 s every 120 s for at

least 800 min. SiOx/Si samples and the two PnBMA samples were measured for 5 s every 10 s to

allow for better analysis of instrument and film thickness stability and were only measured for

aging time of 80 min due to the stability of the thickness of the samples. To prevent the uptake of

water into the PnBMA samples, I continuously flowed dry nitrogen gas over the sample

throughout the aging experiments [8]. To mimic conditions for bilayer samples, dry nitrogen gas

was flowed over one run of a bulk PS film. Ellipsometry measurements of $\Psi(\lambda)$ and $\Delta(\lambda)$ were fit

for λ=400-1000 nm to a layer model corresponding to the sample type.

2.2.1: Verifying instrument stability with 1000 nm SiO_2/Si Substrates

In order to verify instrument stability, I performed multiple control runs on a piece of silicon with a 1000 nm thermal oxide layer (SiO_2/Si). Because SiO_2/Si has an extremely high glass transition temperature, compared to the temperature range (20 – 120 ℃) I am using, the sample responds almost instantaneously to changes in temperature and experiences no physical aging. The layer model for SiO_2/Si consisted of a thermal oxide layer atop of a silicon substrate, called "SiOx_aging" in CompleteEase software. Only the thickness of the thermal oxide layer is fit for this layer model. Plots of temperature and normalized oxide layer thickness, $h(t)/h_p$, versus time, t, are shown in Figure 5. To enable comparison between runs, each data set was normalized to its plateaued thickness value, h_p. This value was obtained by averaging the thickness measurements between 50 min and 80 min on the original time scale, where the thickness remained most constant. This normalization was done to accommodate slight variations in absolute thickness each time the ellipsometer was realigned. The measured temperature for each run is shown as solid lines, and the thickness measurements are shown as individual data points. I defined time t=0 min as the first point at which the temperature was measured to be stable at the desired aging temperature and remained at that aging temperature for the rest of the run. The data was then shifted according to this new time scale. I performed this control experiment three times on different days to ensure the instrument stability responds the same way each time. Over the three runs, the measured temperature profile remained identical, mimicking the setpoint temperature profile almost exactly. This consistency indicated the heater was accurately following the specified temperature profile.

To focus on the data I was most interested in, Figure 5(b) plots the portion of Figure 5(a) within the red dashed box. As can be seen from part (b) of Figure 5, the SiO_2 layer thickness measurements stabilize approximately 10 min after t=0 min. After 10 min, the normalized

thickness measurements from the three runs stabilized and remained at that value for the remainder of the run. Since there should be no change in thickness when the temperature remains constant, this stability in normalized thickness values indicates the ellipsometer can reliably measure changes in thickness, and, since the changes in thickness for the physical aging measurements will be quite small, any change in thickness values can be attributed to actual changes in thickness of the sample instead of instrument noise.
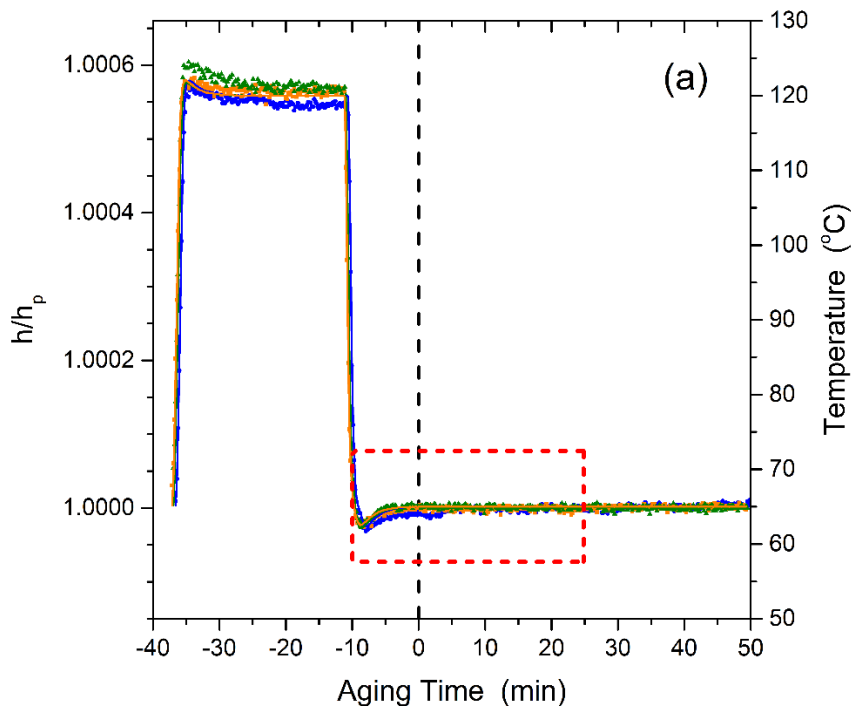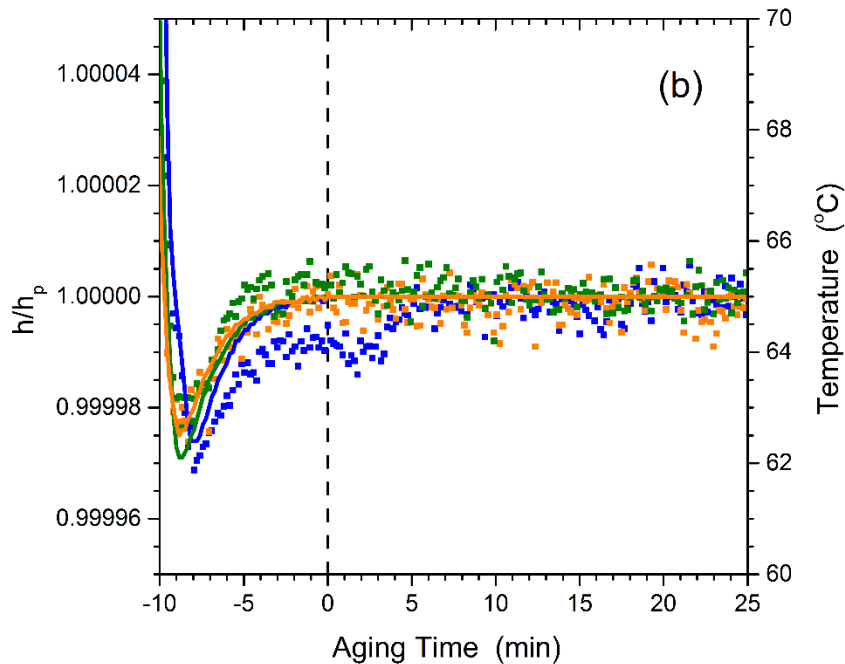
Figure 5. Normalized film thickness of 1000 nm SiO_2 layer, $h(t)/h_p$, and measured heater temperature plotted as functions of time during the temperature profile used for physical aging measurements to test instrument stability. Temperature curves are represented with solid lines, while normalized thickness data are shown as symbols. (a) displays the entire temperature profile, while (b) focuses on the region indicated by the red-dashed rectangle in (a), to display the stabilization of temperature and thickness measurements.

2.2.2: Polystyrene (PS) Bulk Films

To ensure I was performing proper aging measurements, I measured the aging rate, β, of several bulk PS films, using the temperature profile outlined previously. The layer model for PS samples was a Cauchy layer model, $n(\lambda) = A + \frac{B}{\lambda^2} + \frac{C}{\lambda^4}$, for the PS layer, where A, B, C and the film thickness, h, were fit, atop a 1.25 nm native oxide layer as part of the silicon substrate [2], as

discussed in Section 1.2. Figure 6 graphs the normalized film thickness $h(t)/h_0$ versus log(time). Each set of data is collected from a different sample on a different day. As with 1000 nm SiO_2/Si, $t=0$ min was defined to be the first time at which the sample reached the aging temperature of 65 $^{\circ}C$ and remained at that temperature. The data were normalized to the thickness h_0 value at 10 min, which was found by averaging the thickness values of the sample from $t = 5$ min to $t = 15$ min, so normalized thickness was h/h_0. The initial thickness was used following the procedure developed by Baker et al. [3]. The aging rate β was found by doing a linear fit over the graph of normalized thickness versus log(time), only fitting the section of the graph which was linear [9]. Polystyrene aging runs can be successfully performed without flowing dry nitrogen gas over the sample, so most of these samples measured were done without nitrogen gas. However, since nitrogen gas will be required in the aging runs of PnBMA/PS bilayer films, one run was done with dry nitrogen gas to ensure consistency with data collected without dry nitrogen gas. In Figure 6, one data set is from a run without dry nitrogen gas, and the other had dry nitrogen gas. From the overlapping of the data, it is clear dry nitrogen gas does not affect the aging rate of PS. I measured aging rates of 9.48 x 10^{-4}, 9.97 x 10^{-4} and 9.63 x 10^{-4}, which agree with known values for the aging rate of bulk PS at 65 $^{\circ}C$ [9]. This agreement confirms that I am properly measuring the physical aging rate, increasing confidence in other aging measurements done in this thesis.
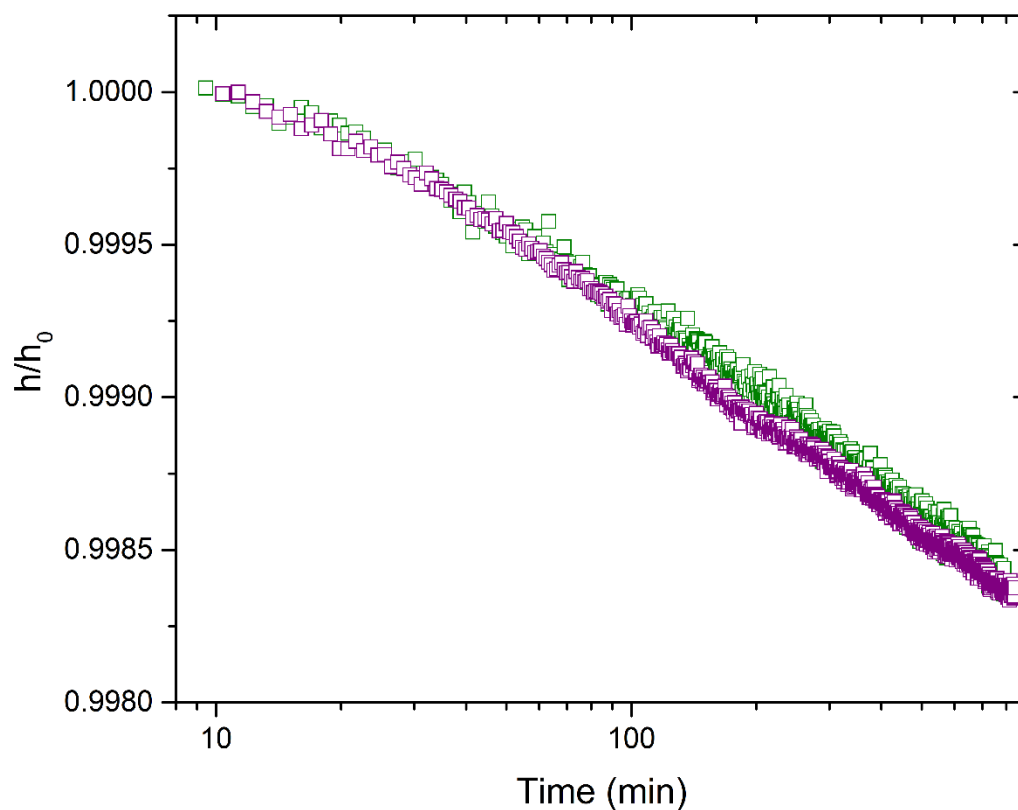
Figure 6. Normalized thickness h/h_0 vs. log(time) for two bulk PS films supported on silicon of thickness 582 nm (green) and 441 nm (purple). The aging run shown in purple was done with dry nitrogen gas flowing over the sample to mimic bilayer film conditions. Measured aging rates correspond to literature aging rates of bulk PS films at 65 $^{\circ}$C aging temperature.

2.2.3: Poly(*n*-butyl methacrylate) (PnBMA) Bulk Films

I studied the stability of several bulk PnBMA films of thickness 390-430 nm supported on silicon as they went through the same temperature profile previously described in Section 2.2 to be used for the physical aging measurements. Following the analysis procedure developed by Rauscher et al. [8], I will be holding the PnBMA layer thickness constant during the layer model

fitting of PnBMA/PS bilayers to determine the physical aging rate of the PS layer. Thus, these control measurements on PnBMA are to confirm that holding the PnBMA layer thickness constant is a valid approximation. The PnBMA samples were prepared via the procedure outlined in 2.1. The layer model for PnBMA samples was a Cauchy layer model, $n(\lambda) = A + \frac{B}{\lambda^2} + \frac{C}{\lambda^4}$, for the PnBMA layer, where A, B, C and the film thickness, h, were fit, atop a 1.25 nm native oxide layer as part of the silicon substrate. Data were normalized in the same manner as PS bulk films, and t=0 min was defined the same way as for the SiO_2. To find at what point I could begin using data, I analyzed Figure 7 in a similar manner to what was done in Section 2.2.1 with the 1000 nm SiO_2/Si samples. Part (a) of Figure 7 shows the entire quench procedure and the first 50 min of aging as normalized thickness $h(t)/h_p$ versus time, where, again, the data were normalized to the thickness value h_p that the film stabilized to at long times (50 to 80 min). Part b of Figure 7 illustrates that PnBMA reaches a stable thickness 10 min after t=0 min. This is faster than was reported by Rauscher et al. [8]. We believe this is because the temperature quench is now performed directly on the ellipsometer where dry nitrogen gas can be flowed through the sample chamber continuously. In contrast, Rauscher et al. [8] annealed and quenched the films off the ellipsometer, only placing the sample on the ellipsometer heater at the start of the aging run. Therefore, for the physical aging of PS layers, h_0 can be taken to be the average of the PS layer thickness at a time of 10 min (± 5 min), and all data prior to that time is discarded

for aging analysis, as is done for single layer PS films normally.
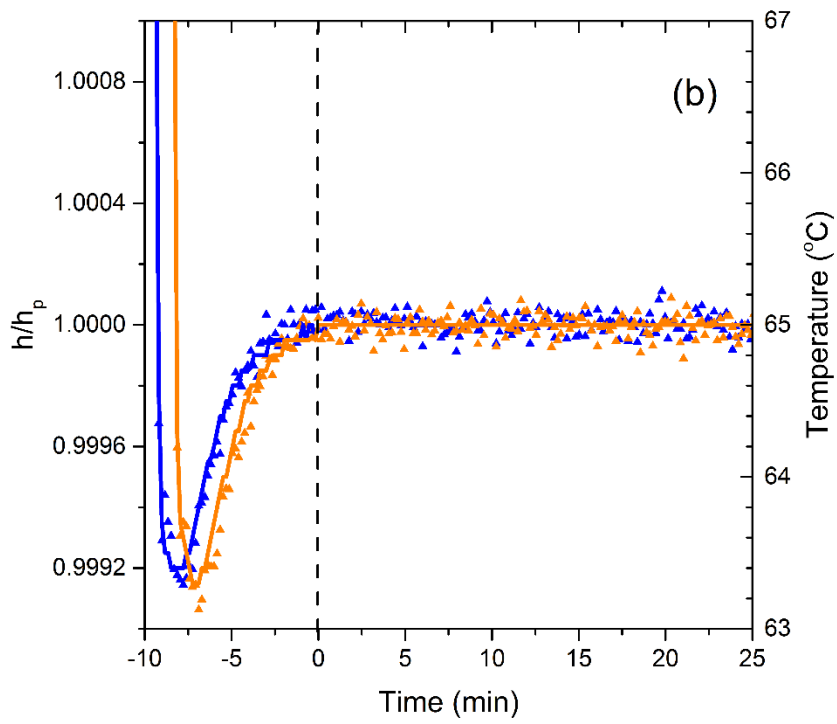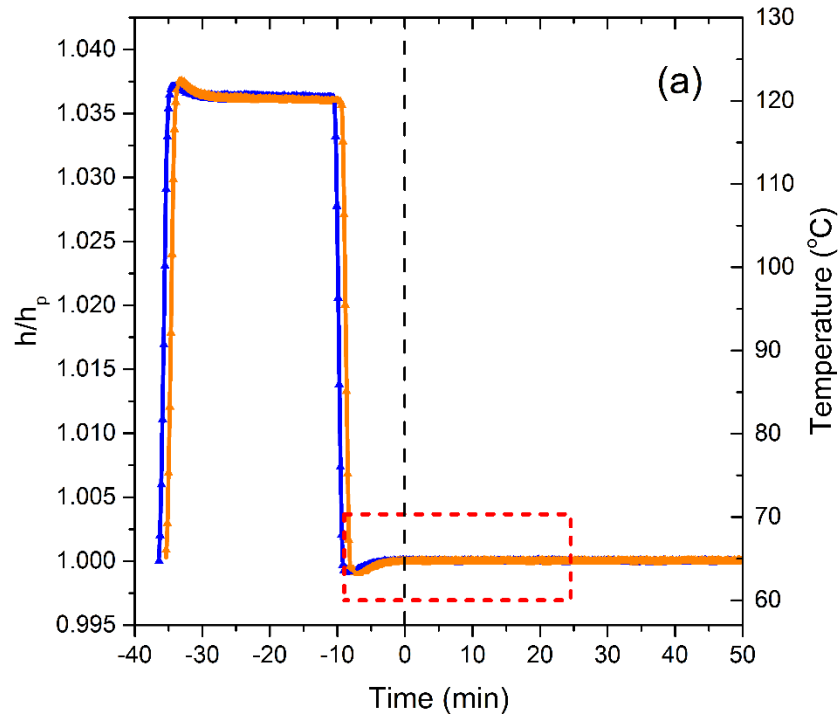
Figure 7. Measuring PnBMA bulk film stability. Part (a) shows the quench and first 50 min of aging data of normalized PnBMA film thickness h/h_p versus log(time) for bulk PnBMA films. Part (b) shows only the first 25 min of data after the quench to highlight when PnBMA films stabilize after being cooled to 65 °C.

Since 65 °C is above the glass transition temperature $T_g = 20$°C for PnBMA, there should be no aging, meaning the PnBMA film thickness would stay constant over the entire aging run. Figure 8 shows data for both PS and PnBMA films as normalized film thickness $h(t)/h_0$ versus log(time). During the aging run, there is some small variation in PnBMA thickness, but this is small in comparison with the thickness decrease observed in the PS films due to physical aging. This stability implies that any change in the total thickness of the PS/PnBMA bilayer films will be due to the change in the thickness of the PS layer, not the PnBMA layer. Therefore, I will be able to measure the aging rate of the PS layer in the bilayer film simply by measuring the aging rate of the entire film.
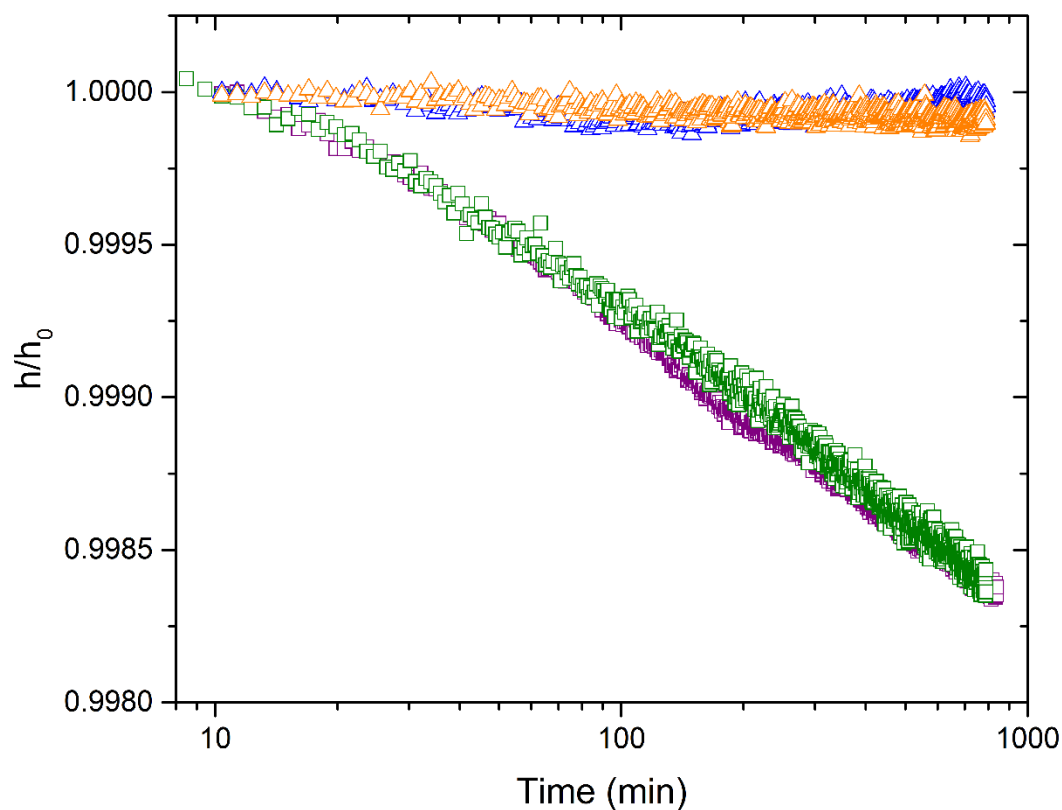
Figure 8. Normalized film thickness h/h_0 vs log(time) comparing bulk PS and bulk PnBMA films. PS films are shown as green and purple squares (same data as shown in Figure 6), while PnBMA films are shown as orange and blue triangles. Compared to PS films, the PnBMA films remain at constant thickness throughout the aging run, implying I can consider the PnBMA layer to remain at constant thickness in bilayer films and any change in thickness will be due to the PS layer.

2.2.4: PnBMA/PS Bilayer Films

I measured PnBMA/PS bilayer films to observe how the physical aging rate of the PS layer was changed by the presence of the adjacent rubbery PnBMA layer. The layer model for

these samples consisted of a 1.25 nm SiOx layer atop the silicon, all below a PS layer. On top of

the PS layer was a 7 nm interfacial layer [8] and on top of that layer was a PnBMA layer. Initial

measurements were done with both PnBMA and PS layers of bulk thicknesses. Multiple different

thickness combinations were done for these measurements. First, a combination of 700 nm of

PnBMA atop 560 nm of PS was chosen because both layers were safely in the bulk regime of

thickness. Next, a combination of 470 nm of PnBMA atop 380 nm of PS was used to observe the

system with the layers closer to the lower bound of the bulk regime. The final bulk samples were

composed of 400 nm of PnBMA atop 300 nm of PS. All subsequent measurements were done

with PnBMA layers of thickness of approximately 400 nm and decreasing thicknesses of the PS

layer. Data were analyzed using the same two fitting methods used by Rauscher et al. [8],

discussed in section 1.7, and all thicknesses were normalized to h_0 values at 10 min found by

averaging the thicknesses from $t = 5$ min to $t = 15$ min. All bilayer data, including fitting

methods will be discussed in Chapter 3.

Chapter 3: Results and Discussion

3.1: Bulk PnBMA/PS Bilayers

The bilayers consisting of 700 nm PnBMA atop 560 nm PS were analyzed with the same two fitting methods used by Rauscher et al. [8] to compare the two techniques. As discussed in section 1.7, the first fitting method ("Fit All") fit 6 parameters: A and B of the Cauchy model, along with the layer thickness for both PnBMA and PS. This fitting method yielded $\beta = 9.55$ x 10^{-4}, $\beta = 9.94$ x 10^{-4} and $\beta = 10.4$ x 10^{-4} for three different bilayer samples of similar layer thicknesses, all of which agree with bulk physical aging rate values found for single layer PS films in Section 2.2.2. The second fitting method held A and B of the Cauchy model, along with the thickness of the PnBMA layer constant at initial values and only fit A and B of the Cauchy model and the thickness of the PS layer. The initial values for the PnBMA layer were found by averaging the values found in the 6-parameter fitting method from $t = 5$ min to $t = 15$ min. The 3-parameter method produced $\beta = 9.80$ x 10^{-4}, $\beta = 9.67$ x 10^{-4} and $\beta = 10.5$ x 10^{-4} for the same set of samples as the 6-parameter fit. As can be seen from the β values and in the representative graph in Figure 9, for a given data set, the two methods are in agreement, yielding similar values of β.
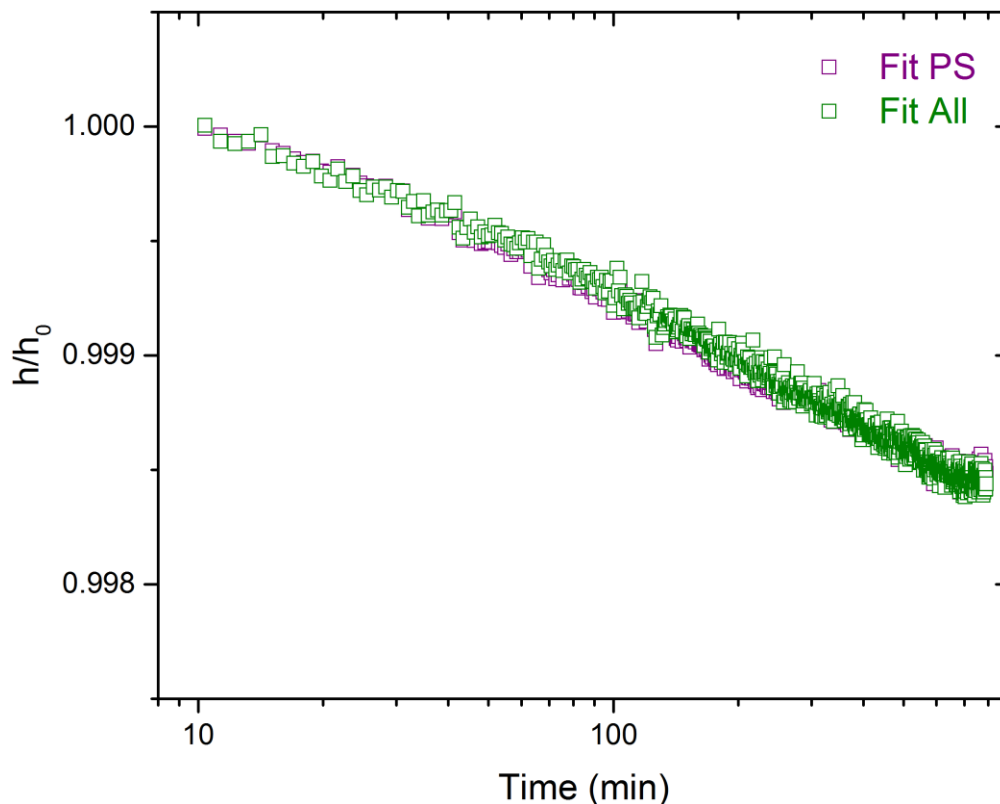
Figure 9. Single data set fit with both the 6-parameter fitting method ("Fit All") (green) and the 3-parameter fitting method ("Fit PS") (purple). Both methods agree, as can be seen in the overlap in the green and purple data. The 6-parameter fitting method yielded a physical aging rate of β = 9.55 x 10^{-4}, while the 3-parameter fitting method yielded a physical aging rate of β = 9.80 x 10^{-4}.

Since the two fitting methods produced similar physical aging rates, I looked closer at the various parts of the fits to further evaluate each method. Figure 10 shows a comparison of the PS and PnBMA layer data for each fitting method. As can be seen from the top row of panels in Figure 10, the 6-parameter fitting method has more noise, especially for the PnBMA data. Since my data on single layer PnBMA films showed the thickness of the PnBMA layer is constant

throughout the aging protocol and the data of the PnBMA layer in the bilayer films also shows constant thickness over the aging run, the values of the PnBMA layer could be held fixed at the initial values. The bottom row of panels in Figure 10 shows that the 3-parameter fitting method has less noise while still being accurate, so the 3-parameter method was used for the rest of this work.
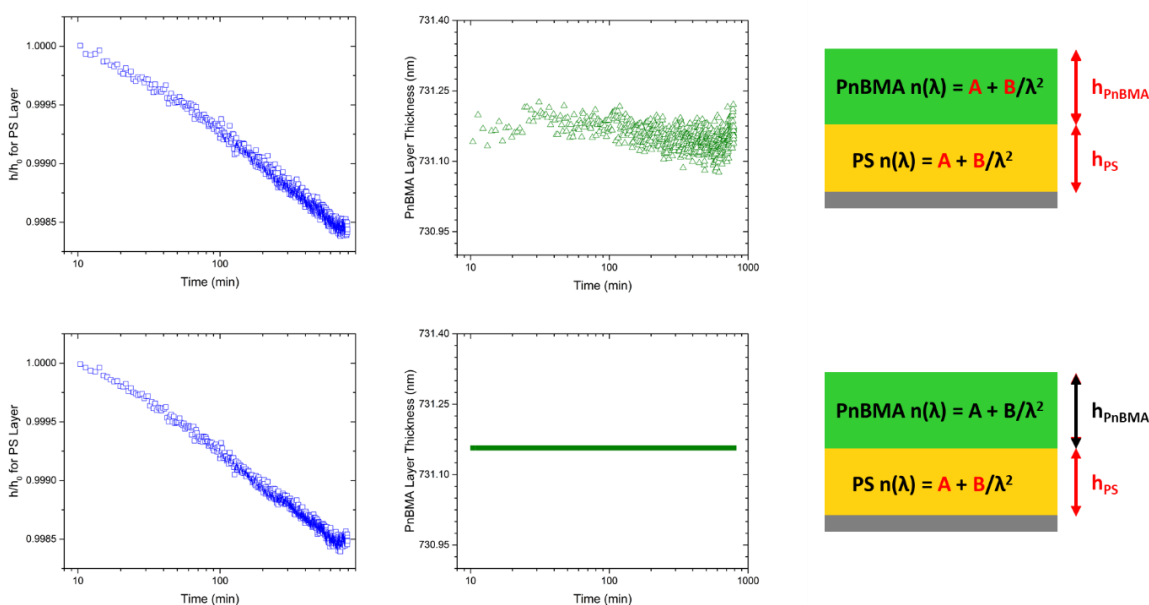
Figure 10. Comparison of 6-parameter and 3-paramter fitting methods. The top row of the figure, showing data for the 6-parameter fit, shows that the PnBMA layer thickness remains constant throughout the run, as agrees with previous single layer PnBMA data. The 3-parameter fitting method shown in the bottom of the figure has less noise, while still giving results in agreement with the 6-parameter fitting method.

700 nm PnBMA/560 nm PS bilayers yielded physical aging rates in agreement with those of bulk single layer PS. However, the goal of this project is to study how the physical aging rate

changes as the PS layer thickness decreases. Based on the work of Baglay and Roth [6] there

might be a change in physical aging rate starting at a PS layer of thickness 250 nm, but single

layer films do not see a change in physical aging rate until they are less than 100 nm [5].

Therefore, to fully study the effect of the PnBMA layer on the PS layer, I need to decrease the

PS layer thickness as much as possible. The extent to which I can decrease the PS layer is

determined by the overall thickness of the film and the ability of the ellipsometer to accurately

measure the thickness of the PS layer. As the percentage of the film consisting of PS decreases,

the ability of the ellipsometer to measure the thickness of the PS layer decreases. Therefore, if I

were to use a PnBMA layer of 700 nm, it would be unlikely I could get an accurate measure of

the physical aging rate of a PS layer of 100 nm. Thus, having confirmed my ability to measure

the physical aging rate of the PS layer within the bilayer films, I was interested in decreasing the

thickness of the PnBMA layer to the smallest possible thickness that was still in the bulk regime.

For my first step in doing so, I decreased the PnBMA layer thickness to 470 nm and the

PS layer thickness to 380 nm. Both of these thicknesses are still safely in the bulk regime. The

exact physical aging rates for the two samples done at this thickness were $\beta = 9.35 \times 10^{-4}$ and $\beta =$

10.4×10^{-4}. Unsurprisingly, these samples produced aging rates in agreement with the 700 nm

PnBMA/560 nm PS samples. To minimize the thickness to which the PS layer could be

decreased and still be able to measure its physical aging rate, I decreased the PnBMA layer

thickness even further to 400 nm with a 300 nm PS layer. The physical aging rates of these

samples were $\beta = 10.7 \times 10^{-4}$ and $\beta = 10.3 \times 10^{-4}$, which was, again, in agreement with data from

the 700 nm PnBMA/560 nm PS samples and the 470 nm PnBMA/380 nm PS samples. All data

with PnBMA layers with thicknesses of at least 400 nm and PS layers with thicknesses of at least

280 nm were considered bulk data. Figure 11 shows a compilation of all bulk data, which had

physical aging rates ranging from $\beta = 9.35$ x 10^{-4} to $\beta = 10.7$ x 10^{-4}.
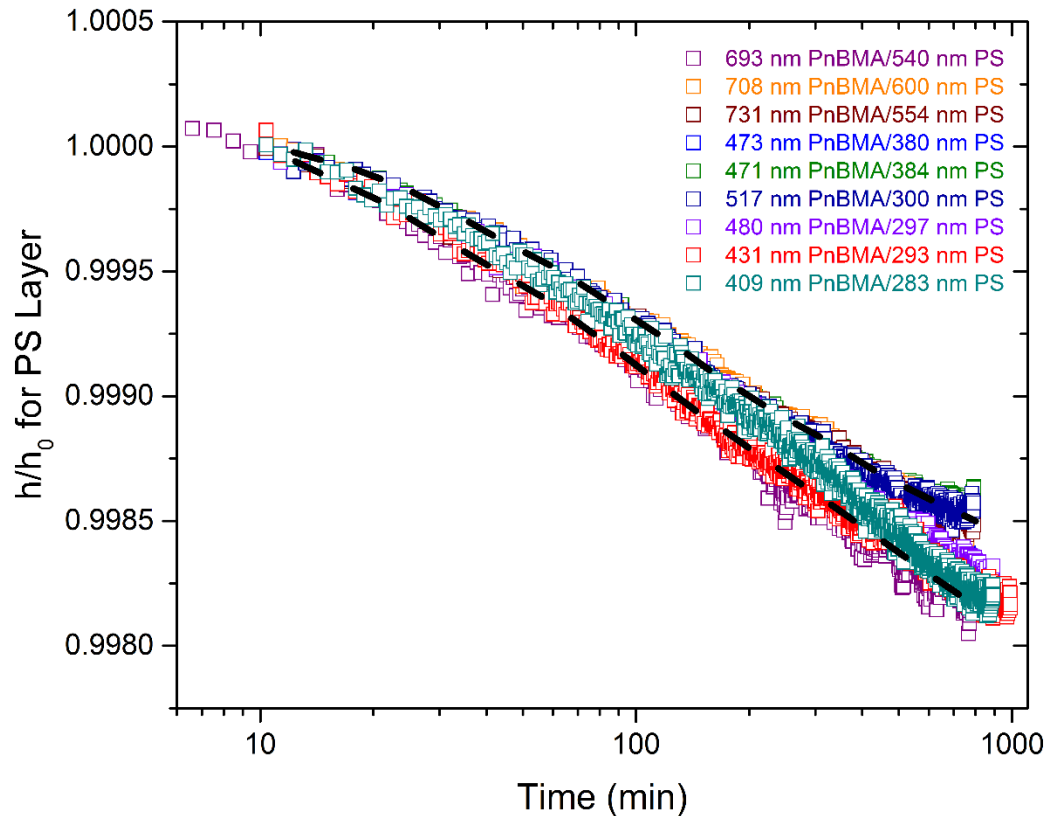
Figure 11. All bulk bilayer data. Physical aging rates ranged from $\beta = 9.35$ x 10^{-4} and $\beta = 10.7$ x

10^{-4}. Samples with PnBMA layers with thicknesses of at least 400 nm and PS layers with

thicknesses of at least 280 nm were considered bulk data. The dashed black lines represent the

range of bulk data

While testing bulk data, I additionally did tests to verify no trace amounts of water were

remaining in the bilayer samples after floating. Since water can plasticize polymers and

plasticization is known to eliminate confinement effects [10], this was good to address. To do so,

I tested two different annealing protocols. The first, described in section 2.1, annealed PS layers at 120 °C and PnBMA layers at 70 °C each separately for at least 18 hours prior to assembling the bilayer via floating. The only annealing done after floating was during the beginning of the aging protocol described in section 2.2, when the sample was heated to 120 °C for 30 minutes. To test if 30 min at 120 °C was sufficient to remove water from the sample, I used a second protocol in which I assembled the bilayer immediately after spin-coating and annealed the entire bilayer at 80 °C for at least 18 hours under vacuum before the final annealing done on the ellipsometer. This protocol ensured no water remained in the sample when aging measurements were done.

To test the differences in annealing protocols, I measured two samples of identical layer thicknesses, one of which was annealed using the first protocol (before floating) and the other was annealed using the second (after floating). These samples had a PnBMA layer thickness of 400 nm and a PS layer thickness of 300 nm. Both samples produced aging rates within the range of other bulk data, indicating that annealing protocol does not affect the samples. The agreement of these two samples can be seen in Figure 12 in the overlap of the two data sets.
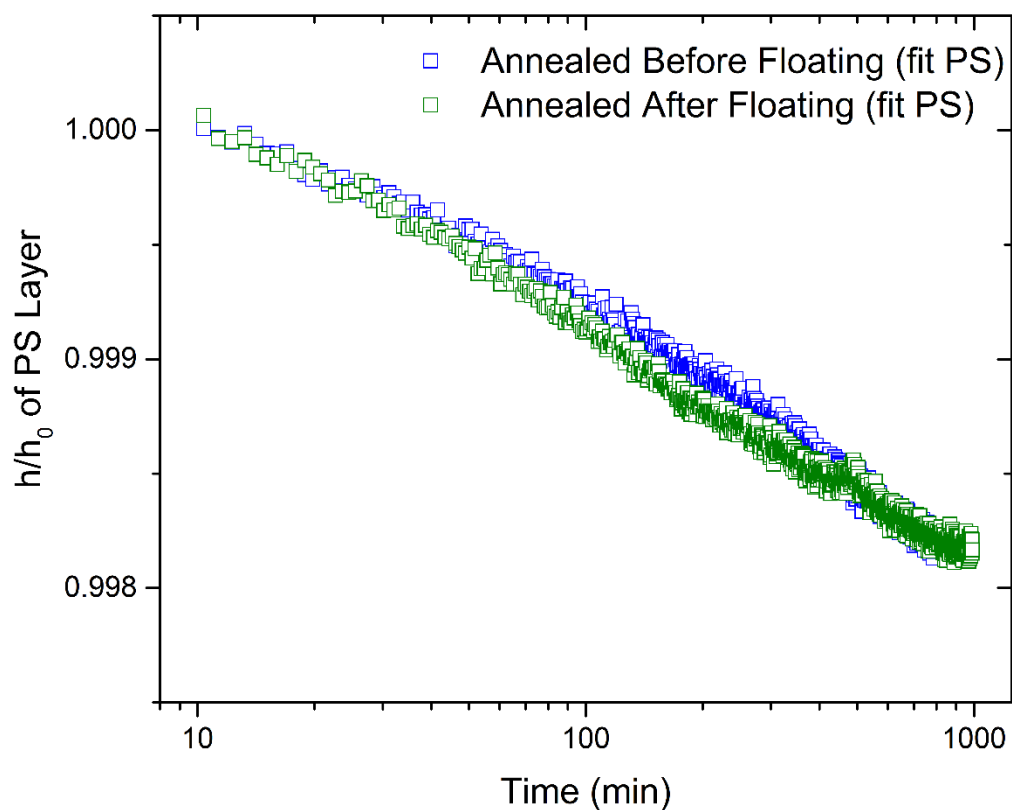
Figure 12. Comparison of annealing protocols for 400 nm PnBMA/300 nm PS samples. Annealing after floating was done to ensure any water remaining in the sample after floating was removed. The overlap of the data sets and similarities in physical aging rates confirmed there was no remaining water in the samples during either sample preparation procedure.

To further confirm there was no water remaining in the samples after floating I made two samples of PnBMA spin-coated onto silicon and two samples of PnBMA floated onto silicon and measured the thicknesses before and after annealing at 80 ℃ for 18 hours. All samples had the same thickness before and after annealing and samples spin-coated onto silicon had thicknesses in agreement with samples floated onto silicon. These tests confirm that residual water was not

an issue in the samples. Since both annealing protocols produced similar results, I used the

second annealing protocol, which is experimentally more expedient, where the bilayer is

annealed after floating at 80 ºC for at least 18 hours for the remainder of the data collected.

3.2: 400 nm PnBMA/PS Bilayers—Decreasing PS Layer Thickness

To study the physical aging rate closer to the PnBMA/PS interface, I decreased the PS

layer thickness, while keeping the PnBMA layer a constant 400 nm. Representative data sets of

each PS layer thickness are shown in Figure 13. In Figure 13, the range of the bulk data is

represented by the same black dashed curves as seen in Figure 11.
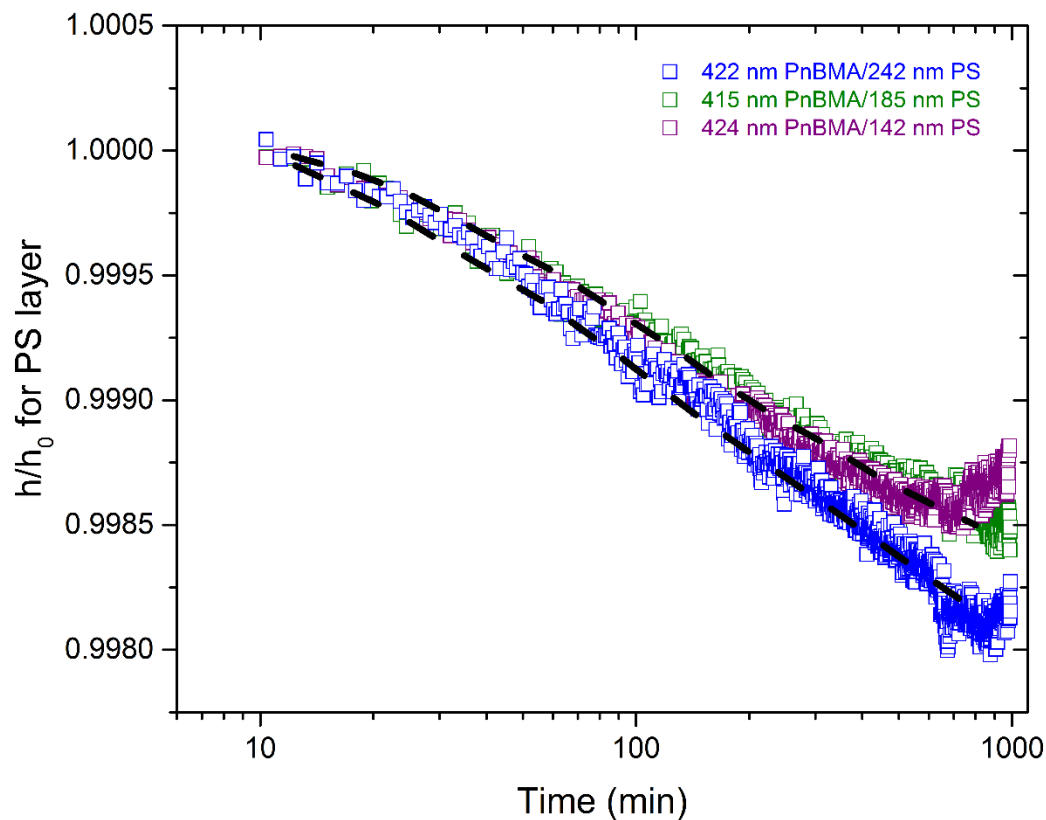
Figure 13. Representative data sets of decreasing PS layer thickness compared to bulk. Bulk data is represented by the black dashed lines, while 242 nm PS layer is in blue, 185 nm PS layer is in green and 142 nm PS layer is in purple. None of these samples deviated from the bulk PS layer data.

As can be seen in Figure 13, PS layers of 242 nm, 185 nm and 142 nm all do not deviate from bulk. Given that single layer PS films do not see a decrease in physical aging until they reach a thickness of 100 nm [5], the agreement with bulk of my bilayer samples with 142 nm PS is not surprising. However, when measurements were attempted on bilayers with PS layers thinner than 142 nm, unreliable data was collected. This was because the PnBMA layer was so much larger than the PS layer that small changes in the thickness of the PS layer could not be reliably measured. Therefore, in order to measure the physical aging rates of PS layers any smaller than 142 nm, a reduction in the thickness of the PnBMA layer was needed.

3.3: PnBMA/150 nm PS Bilayers—Decreasing PnBMA Layer Thickness

Because the last reliable measurement of physical aging was done on a sample with 142 nm PS, I reduced the thickness of the PnBMA layer down to 150 nm, so my next measurements were done on bilayers with 164 nm PnBMA/146 nm PS and 164 nm PnBMA/145 nm PS. Figure 14 shows a comparison of this data with both bulk data and 424 nm PnBMA/142 nm PS data, along with 415 nm PnBMA/185 nm PS data. Clearly from Figure 14, 164 nm PnBMA/146 nm PS and 164 nm PnBMA/145 nm PS had approximately the same physical aging rate as that of bulk and previous data. Therefore, a PnBMA layer of approximately 150 nm PnBMA can be used while reducing the thickness of the PS layer further.
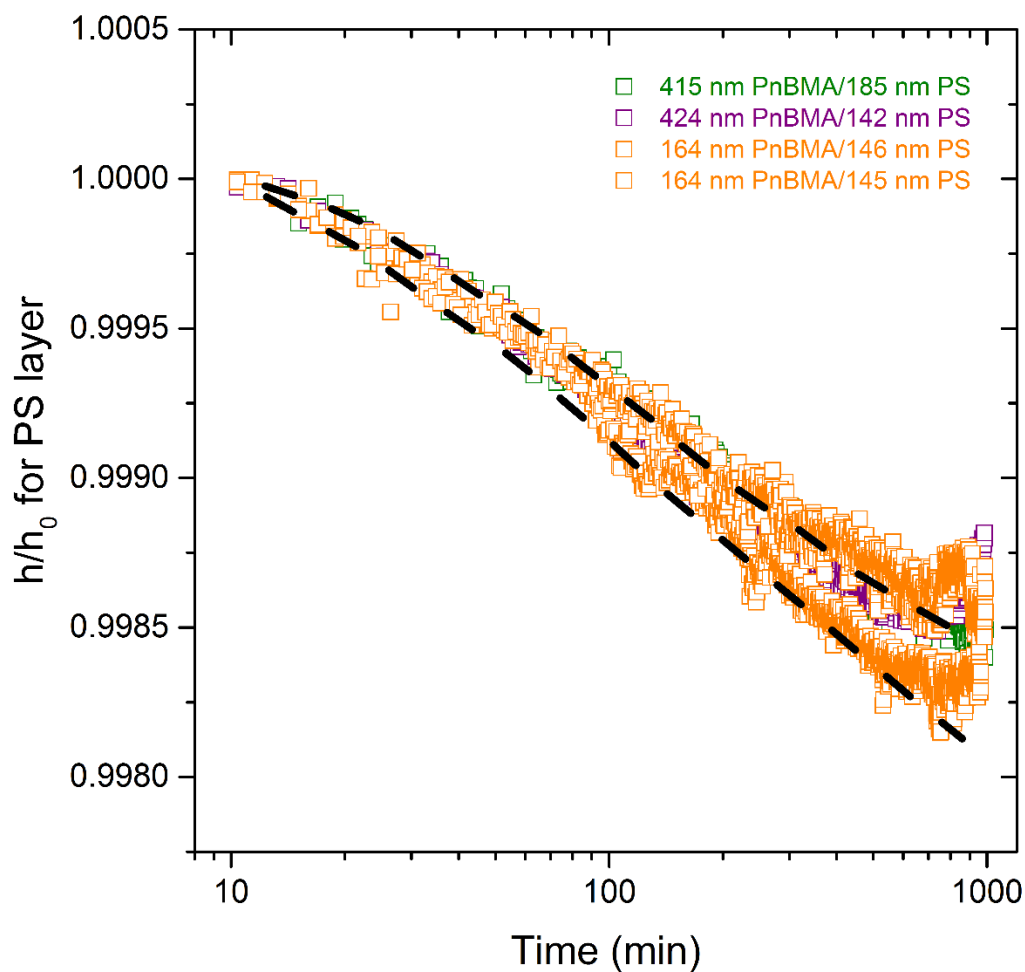
Figure 14. Comparison of 164 nm PnBMA/146 nm PS bilayer and 164 nm PnBMA/145 nm PS bilayer (orange squares) to previous data (green and purple squares). Bulk data is represented by black dashed lines. Since the orange data agrees with previous data, the PnBMA layer can be decreased to 150 nm.

3.4: 150 nm PnBMA/PS Bilayers—Decreasing PS Layer Thickness

In decreasing the thickness of the PS layer underneath a 150 nm PnBMA layer, I tested bilayers with a PS layer of 97 nm and a PS layer of 57 nm. Figure 15 shows the aging data from

these samples in comparison with the 164 nm PnBMA/146 nm PS bilayer data,164 nm

PnBMA/145 nm PS bilayer data and the bulk data outline. The 97 nm PS bilayer clearly

indicates no deviation from bulk. However, the 57 nm PS bilayer begins to increase in
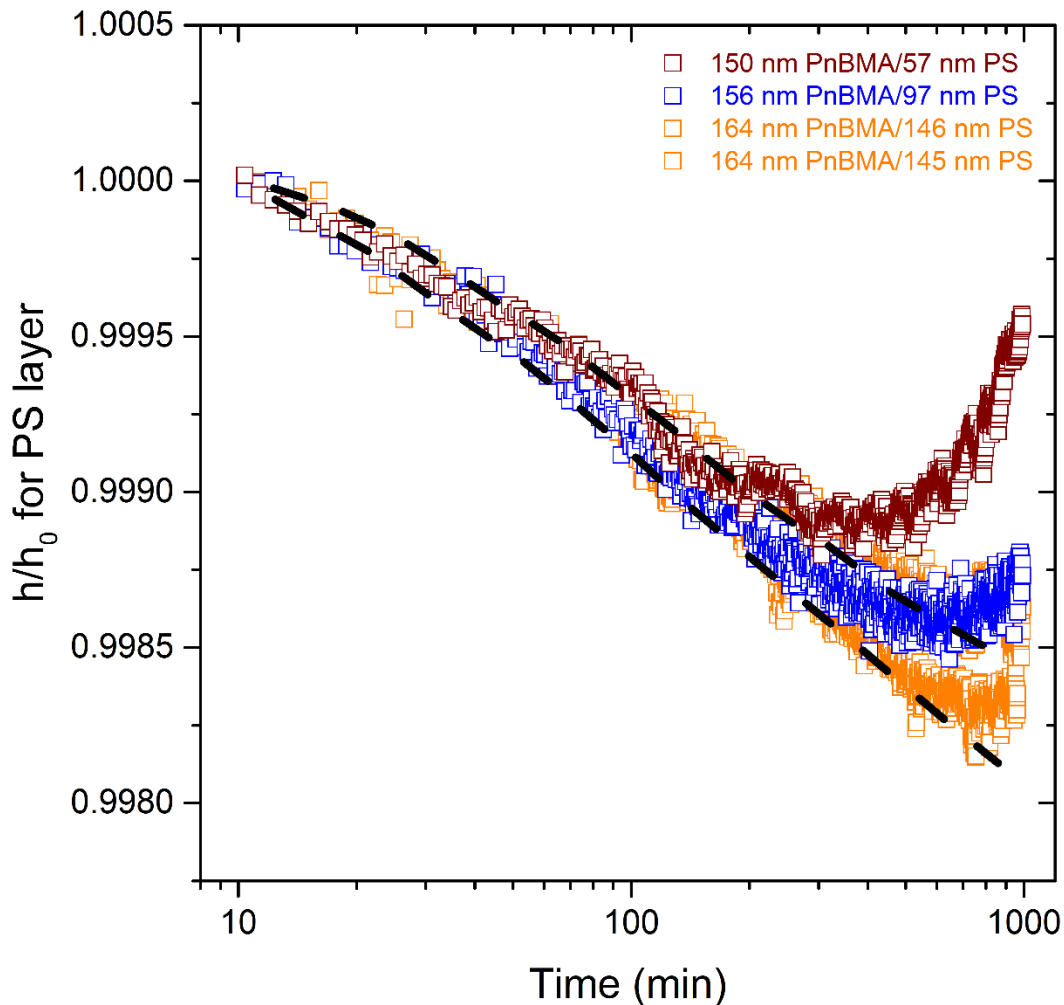
Figure 15. Decreasing PS thickness for a 150 nm PnBMA/PS bilayer. Orange data represents

164 nm PnBMA/145 nm PS. Blue data is for 156 nm PnBMA/97 nm PS, and burgundy data is

for 150 nm PnBMA/57 nm. There is no obvious deviation from bulk data (black dashed lines).

The burgundy curve indicates possible issues with insufficient dry nitrogen gas flow affecting

the stability of the PnBMA layer.

measured normalized thickness at approximately 300-400 min into the aging experiment. This increase in normalized thickness is clearly inconsistent with the definition of physical aging, which dictates that glassy polymers will densify and contract over time while undergoing physical aging. Therefore, this "measured" increase is unlikely to be due to an actual increase in PS layer thickness. The more likely explanation is that the 150 nm PnBMA layer on top of the 57 nm PS layer is expanding or contracting in response to the environment, and the fit model is trying to account for that change in the PS layer thickness. Since the PnBMA layer thickness is held constant in the 3-parameter fitting method, any change in PnBMA layer thickness must be attributed to the PS layer in this model. Thus, in this scenario, the PnBMA layer likely expanded in response to environmental factors, for example, a change in room humidity, so the fit model accounted for that expansion by increasing the thickness of the PS layer. I also saw slight increases in normalized film thickness for other bilayer samples towards the end of aging runs. All of these increases occurred within the last 200-300 minutes of aging experiments when the decrease in thickness due to aging becomes small and is observed to be more prominent as the ratio of PS layer thickness to PnBMA layer thickness decreases. Because these increases only occurred when the PnBMA layer was much larger than the PS layer, I concluded that the increase was due to the rubbery PnBMA layer responding to changes in the environment. While I attempted to keep the PnBMA layer constant by flowing dry nitrogen gas over the sample throughout the aging experiments, this sensitivity of the PnBMA layer indicates I was likely not flowing a sufficient amount of nitrogen gas over the sample to make it resistant to environmental changes. Increasing the flow rate of dry nitrogen gas over the sample in future experiments could make the PnBMA layer more resistant to changes in the environment. Changing the time of day the aging experiment was started did not change the behavior of the aging data, and increases

were still seen at approximately the same amount of time into the aging run. Additionally, I tried

fitting the data with all 6 parameters and saw that the PnBMA layer thickness still remained

noisy and flat. The lack of change resulting from these tests indicates we need to do more work

to fully understand what is causing these presumably artificial increases in PS layer thickness

and how to correct it.

Regardless of the upturn seen in Figure 15, it appears that there is still likely no deviation

from bulk in the physical aging rate for a 57 nm PS layer. This lack of apparent change in

physical aging at first seems surprising, given that, for the semi-infinite PS/PnBMA system,

Baglay and Roth saw a reduced T_g up to 250 nm into the PS side [6]. The lack of change in

physical aging that I observed could indicate a shortening of the length scale of the gradient in

dynamics due to the finite boundary conditions in my system. In a later work, Baglay and Roth

found that for systems with finite PS layer size, the gradient in dynamics was altered [11]. We

know from Ellison and Torkelson's work that single layer PS films begin to experience a

reduction in their gradient in dynamics when the total film thickness becomes less than 60 nm

[4]. Below 25 nm, one can no longer measure a gradient in dynamics, only an average T_g value

because it is believed the film can no longer support a complete gradient in dynamics [4]. It

would be reasonable to hypothesize that confinement of the PS layer to a finite size could affect

the gradient in dynamics in my bilayer system as well. Therefore, it is entirely possible the

gradient in dynamics caused by the glassy-rubbery interface is not as long as one might infer

from the original Baglay and Roth work [6].

Chapter 4: Conclusion

I measured the physical aging rate of a glassy PS layer adjacent to a rubbery PnBMA layer to see how the glassy-rubbery interface affected the physical aging of the PS layer. I used a 1000 nm SiO_2/Si substrate to measure instrument stability, bulk PS samples to test for agreement with the literature, and bulk PnBMA samples to test that the PnBMA thickness remained constant throughout aging experiments. The fact that the PnBMA thickness remains constant throughout the aging experiments allowed the physical aging rate of the PS layer to be found by measuring the changes in thickness of the overall bilayer. I measured PnBMA/PS bilayers with PnBMA layers ranging in thickness from 400 nm to 700 nm and PS layers ranging in thickness from 300 nm to 600 nm to establish a range for physical aging of bilayers with PnBMA and PS layers of bulk thickness. I then decreased the thickness of the PS layer while keeping the PnBMA layer at a constant thickness of 400 nm. Due to a difficulty in measuring bilayers with a PS layer smaller than 142 nm, I decreased the PnBMA layer to 150 nm, while keeping the PS layer at a thickness of 150 nm. Seeing no change in physical aging rate with a reduced PnBMA layer thickness, I proceeded to decrease the thickness of the PS layer down to 57 nm below a 150 nm PnBMA layer.

There was no change in physical aging of the glassy layer of the bilayer film down to PS layers of 142 nm. Given that there is no change in physical aging of single layer PS films down to 100 nm [5], this was not entirely surprising. I have also changed the boundary conditions, which changes the scale of the T_g profile, so the length scale of perturbation in this system is likely smaller than that seen by Baglay and Roth [6, 11]. To fully understand the effect of the adjacent rubbery layer on the physical aging of the glassy PS layer, I would need to further decrease the thickness of the PS layer. However, a PnBMA layer of 400 nm cannot be used to do

so. I confirmed that a PnBMA layer of 150 nm produces the same results as a PnBMA layer of 400 nm, so the remainder of my work could use a PnBMA layer of 150 nm and a PS layer of decreasing thickness to study the effect of an adjacent rubbery layer on the glassy PS layer. Decreasing the PS layer, again, showed no deviation from bulk, and emphasized possible environmental influences on the PnBMA layer of the bilayer samples. The influence from the ventilation system was tested by altering the start time of aging experiments. The lack of observed deviation from bulk even down to a PS layer of 57 nm might be explained by a reduction in the length scale of the gradient in dynamics profile, caused by the system, specifically the PS layer, being of finite thickness.

Future work should address influences from the environment and test increased flow rates of dry nitrogen gas over the sample to see if the sensitivity of the PnBMA layer to the environment can be reduced. Once reduction in the PnBMA layer's sensitivity to the environment is accomplished, further reduction in PS layer thickness should be studied. Further future work would include studying the local T_g in the same sample geometry as used in this work, should a change in physical aging rate be observed. Since the length scale of the change in T_g is affected by the sample geometry, studying the T_g profile of this geometry would help us further understand our results here.

References

1.   J.M. Hutchinson, "Physical Aging of Polymers," *Prog. Polym. Sci* **1995**, 20, 703-760.

2.   X. Huang and C.B. Roth, "Changes in the Temperature-Dependent Specific Volume of Supported Polystyrene Films with Film Thickness," *Journal of Chemical Physics* **2016**, 144, 234903.

3.   E.A. Baker, P. Rittigstein, J.M. Torkelson, C.B.Roth, "Streamlined Ellipsometry Procedure for Characterizing Physical Aging Rates of Thin Polymer Films," *Journal of Polymer Science: Part B: Polymer Physics* **2009**, 47, 2509-2519.

4.   C.J. Ellison, J.M. Torkelson, "The distribution of glass-transition temperatures in nanoscopically confined glass formers," *Nature Materials* **2003**, 2, 695-700.

5.   J.E. Pye, K.A. Rohald, E.A. Baker, C.B. Roth, "Physical Aging in Ultrathin Polystyrene Films: Evidence of a Gradient in Dynamics at the Free Surface and Its Connection to the Glass Transition Temperature Reductions," *Macromolecules* **2010**, 43, 8296-8303.

6.   R.R. Baglay, C.B. Roth, "Communication: Experimentally determined profile of local glass transition temperature across a glassy-rubbery polymer interface with a Tg difference of 80 K," *The Journal of Chemical Physics* **2015**, 143, 111101.

7.   D.F. Siqueira, D.W. Schubert, V. Erb, M. Stamm, J.P. Amato, "Interface thickness of the incompatible polymer system PS/PnBMA as measured by neutron reflectometry and ellipsometry," *Colloid Polym Sci* **1995**, 273, 1041-1048.

8.   P.M. Rauscher J.E. Pye, R.R. Balay, C.B. Roth, "Effect of Adjacent Rubbery Layers on the Physical Aging of Glassy Polymers," *Macromolecules*, **2013**, 46, 9806-9817.

9.   M.F. Thees, C.B. Roth, in preparation.

10.   C.J. Ellison, R.L. Ruszkowski, N.J. Fredin, J.M. Torkelson, "Dramatic Reduction of the Effect of Nanoconfinement on the Glass Transition of Polymer Films via Addition of Small-Molecule Diluent," *Phys. Rev. Lett.*, **2004**, 92, 119901.

11.   R.R. Baglay, C.B. Roth, "Experimental Study of the Influence of Periodic Boundary Conditions: Effects of Finite Size and Faster Cooling Rates on Dissimilar Polymer-Polymer Interfaces," *ACS Macro Letters,* **2017**, 6, 887-891.